



UNIVERSITY OF GOTHENBURG

Gothenburg University Publications

Far-infrared amide IV-VI spectroscopy of isolated 2- and 4-Methylacetanilide

This is an author produced version of a paper published in:

Journal of Chemical Physics (ISSN: 0021-9606)

Citation for the published paper:

Yatsyna, V. ; Bakker, D. ; Feifel, R. et al. (2016) "Far-infrared amide IV-VI spectroscopy of isolated 2- and 4-Methylacetanilide". Journal of Chemical Physics, vol. 145(104309),

<http://dx.doi.org/10.1063/1.4962360>

Downloaded from: <http://gup.ub.gu.se/publication/242096>

Notice: This paper has been peer reviewed but does not include the final publisher proof-corrections or pagination. When citing this work, please refer to the original publication.

Far-infrared Amide IV-VI spectroscopy of isolated 2- and 4-MethylAcetanilide

Vasyl Yatsyna,^{1,2} Daniël J. Bakker,² Raimund Feifel,¹ Anouk M. Rijs,^{2, a)} and Vitali Zhaunerchyk^{1, b)}

¹⁾*Department of Physics, University of Gothenburg, 412 96 Gothenburg, Sweden*

²⁾*Radboud University, Institute for Molecules and Materials, FELIX Laboratory, Toernooiveld 7-c, 6525 ED Nijmegen, The Netherlands*

(Dated: 18 October 2016)

Delocalized molecular vibrations in the far-infrared and THz ranges are highly sensitive to the molecular structure, as well as to intra- and inter-molecular interactions. Thus, spectroscopic studies of biomolecular structures can greatly benefit from an extension of the conventional mid-infrared to the far-infrared wavelength range. In this work the conformer-specific gas-phase far-infrared spectra of two aromatic molecules containing the peptide -CO-NH- link, namely 2- and 4-MethylAcetanilide, are investigated. The planar conformations with *trans* configuration of the peptide link have only been observed in the supersonic-jet expansion. The corresponding far-infrared signatures associated with the vibrations of the peptide -CO-NH- moiety, the so-called Amide IV-VI bands, have been assigned and compared with the results of DFT frequency calculations based on the anharmonic VPT2 approach. The analysis of the experimental and theoretical data shows that the Amide IV-VI bands are highly diagnostic for the geometry of the peptide moiety and the molecular backbone. They are also strongly blue-shifted upon formation of the NH \cdots O=C hydrogen bonding, which is, for example, responsible for the formation of secondary protein structures. Furthermore, the Amide IV-VI bands are also diagnostic for the *cis* configuration of the peptide link, which can be present in cyclic peptides. The experimental gas-phase data presented in this work can assist the vibrational assignment of similar biologically important systems, either isolated or in natural environments.

^{a)}Electronic mail: a.rijs@science.ru.nl

^{b)}Electronic mail: vitali.zhaunerchyk@physics.gu.se

I. INTRODUCTION

The knowledge about the three-dimensional (3D) structure of biological molecules is highly important, as the structure typically controls biological processes and chemical reactions, molecular recognition and selective binding of ligands, molecular transport properties *etc.* Hence, the development of new or complementary approaches for molecular structural analysis is highly relevant for broadening and deepening our understanding of biological functioning. Infrared (IR) spectroscopy that probes molecular vibrations is a suitable tool to study the molecular structure. In the last decades, mid-IR studies of biomolecular building blocks in combination with quantum chemical calculations were successfully implemented for structural analysis of various biologically important molecules¹. For polypeptides and proteins typically the Amide A (NH stretch) and Amide I-III (C=O stretch and NH bend) mid-IR vibrations are studied, since these vibrations are characterized by strong absorption intensity and are sensitive to the local electrostatic environment of peptide links, as well as the presence of hydrogen bonding *etc.* In contrast, the far-IR vibrations, have delocalized character, which makes them suited for the analysis of global 3D structure of biomolecules. Moreover, the vibrational motions corresponding to weak interactions such as hydrogen bonding and van der Waals interactions are located in the low-frequency far-IR region, enabling their direct studies by means of far-IR spectroscopy². With the development of more efficient radiation sources, spectroscopy in the far-IR (or THz) spectral range becomes more accessible and promising for applications in different research areas, such as studies of the structure and dynamics of peptides and proteins, and the hydration layer around biomolecules.³⁻⁶

Among the early far-IR studies of biologically important molecules it is worth to mention *N*-Methylacetamide (NMA), which contains a peptide link and two alpha carbons, making it the simplest model for a peptide backbone. Based on far-IR spectra and normal mode analysis of NMA⁷, more complex model systems were studied. In particular, the fundamental amide vibrations in the far-IR range, the so called Amide IV-VII bands (see Fig. 1b), were recognized and shown to be characteristic for peptides and proteins⁸⁻¹⁴. These bands are observed in the range of 200-800 cm⁻¹, with Amide V being the strongest one, corresponding to the NH out-of-plane bending motion. Although several early condensed-phase studies had demonstrated that the Amide V bands have a strong sensitivity to the secondary structures

of polypeptides^{9,15}, the subsequent IR studies were mostly focused on the Amide A and Amide I-III bands, mainly because they are amenable to highly accurate theoretical treatment, and are more straightforward to study experimentally. Only few recent far-IR studies were devoted to Amide IV-VII range in the condensed-phase^{4,16-18}, and in the gas-phase¹⁹⁻²³. With the advance of powerful far-IR (THz) radiation sources, and the development of efficient theoretical approaches which enable accurate calculations of low-frequency vibrational motions²²⁻²⁴, far-IR spectroscopy can nowadays serve as a highly informative extension to the well-established mid-IR region for the studies of molecular structure and weak interactions. For example, in the case of Phe-Ala and Phe-Gly dipeptides the far-IR spectra enabled the distinction between two conformations which were not possible to be resolved in the mid-IR²². In the case of Phe-Pro dipeptides²³, the combination of far-IR spectra with *ab initio* molecular dynamics simulations enabled the study of the β - and γ -turn conformations. The most conformer-specific bands in that case were associated with NH out-of-plane bending motions, either as a part of the NH₂ moiety, or the peptide -CO-NH- moiety.

In the current work we study low-frequency peptide moiety vibrations in isolated 2- and 4-MethylAcetanilide (2-MA and 4-MA) molecules. We employ the free-electron laser FELIX, delivering tunable coherent radiation in the far-IR, and the IR-UV ion-dip spectroscopy technique to measure the conformer-specific 2-MA and 4-MA spectra in the gas phase. The experimental measurements have been combined with theoretical calculations to assign the low-frequency vibrations of peptide moiety and to investigate their structure-specificity. The 2-MA and 4-MA molecules are substituted acetanilides (*N*-phenylamides), in which the peptide -CO-NH- moiety links a methyl group with a substituted aromatic ring (methylphenyl group). Two different isomeric configurations were studied, 2-MA and 4-MA (see Fig. 1a). In general, the -CO-NH- moiety can adopt two distinct nearly planar configurations, either *trans* or *cis*. In the case of 4-MA, this results in two geometries (see Fig. 1a), which have a significant difference in energy. In the case of 2-MA, where the substituent methyl group is located next to the acetamide group, steric interactions lead to the existence of the third conformer, with the -CO-NH- moiety of *trans* character, but oriented out of plane with respect to the aromatic ring. This conformation is characterized by a non-zero dihedral angle ($\approx 60^\circ$) between the -CO-NH- moiety and the ring planes, and we call it *trans-op* 2-MA in what follows (Fig. 1a). Moreover, in the *trans-op* conformation of 2-MA the -CO-NH- moiety deviates from planarity by $\approx 10^\circ$ (B3LYP/N07D geometry). Since in proteins deviation

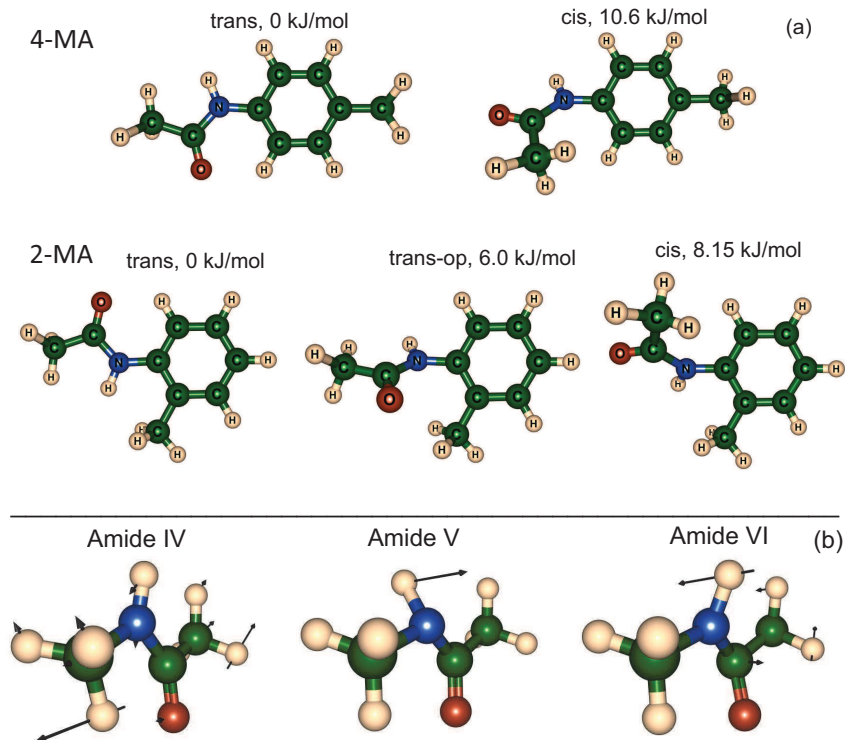


FIG. 1. (a) Geometries and corresponding energies of the 4-MA and 2-MA stable conformations, calculated with the B3LYP functional and N07D basis set. The energy of the conformations is shown with respect to the *trans* ones. (b) Graphical representation of the Amide IV-VI normal modes of NMA, shown with scaled vectors of vibrational displacement. Amide IV vibrations involve CO in-plane bending, CC stretch and CNC deformation; Amide V is mostly NH out-of-plane bending; Amide VI is mostly CO out-of-plane bending with some out-of-plane displacement of the NH group.

from planarity is quite common^{25,26}, the influence of this structural feature on the far-IR spectrum is of great interest.

II. EXPERIMENTAL TECHNIQUE

The mid-IR and far-IR spectra of 4-MA and 2-MA molecules were measured utilizing IR-UV ion-dip spectroscopy²⁷. Briefly, in this technique the molecules are prepared in the electronic- and vibrational-ground state by means of supersonic-jet cooling, and are excited by IR photons and then probed with UV photons. The UV photon energy is selected to

ionize the molecules in form of resonant-enhanced multiphoton ionization (REMPI). Upon the resonant IR excitation the vibronic ground state is depleted, which results in a reduction of the ion signal produced by REMPI. The conformer-specific IR spectra can be measured by scanning the frequency of the IR laser while the frequency of the UV laser is set to the specific REMPI transition of the selected molecular conformation. The 4-MA and 2-MA samples used for the present study were obtained commercially with a stated purity of 99% (Sigma Aldrich) and $> 98\%$ (Apollo Scientific), respectively. A pulsed molecular beam source with a heated sample compartment and heated pulsed valve (Parker general valve Series 9) was used to deliver the molecules into the interaction region. The 4-MA and 2-MA samples were heated to $95\text{ }^{\circ}\text{C}$ and $75\text{ }^{\circ}\text{C}$, respectively, while the temperature of the pulsed valve was kept $5\text{-}10^{\circ}$ higher in order to avoid condensation of the sample in the valve. Argon at high pressure, 3 bar, was used as a carrier gas. After the supersonic jet expansion the coldest part of the molecular beam was selected with a skimmer. Tunable UV radiation was produced by a frequency doubled dye laser (NarrowScan, Radiant Dyes) pumped by a frequency tripled YAG laser (Spectra Physics). The molecular parent ions, generated in the interaction region by a (1+1)-REMPI scheme, were detected with a Jordan reflectron time-of-flight mass spectrometer. The IR light pulses preceding the UV radiation were generated by the free electron laser FELIX operating at 10 Hz. The repetition rate of the UV laser was twice higher (20 Hz), providing reference measurements without IR radiation at every second UV pulse. The IR spectra were measured in the range of $220\text{-}1800\text{ cm}^{-1}$ ($5.5\text{-}45\text{ }\mu\text{m}$) with a FELIX bandwidth of about 1% (FWHM).

III. COMPUTATIONAL DETAILS

Molecular structure optimization and vibrational frequency calculations were performed with the Gaussian 09 package²⁸. The *Tight* optimization criterion (RMS force $< 10^{-5}$) was used in all calculations. Anharmonic spectra of the molecular conformations studied were calculated with a generalized vibrational second-order perturbation theory (VPT2)²⁹ as implemented in Gaussian. In order to increase the accuracy of the frequency calculations, the *Ultrafine* grid (99 radial shells and 590 angular points per shell) was used both for numerical integration and coupled perturbed Kohn-Sham (CPKS) computations. We have chosen the B3LYP density functional and the N07D basis set³⁰ for the VPT2 frequency calculations, as

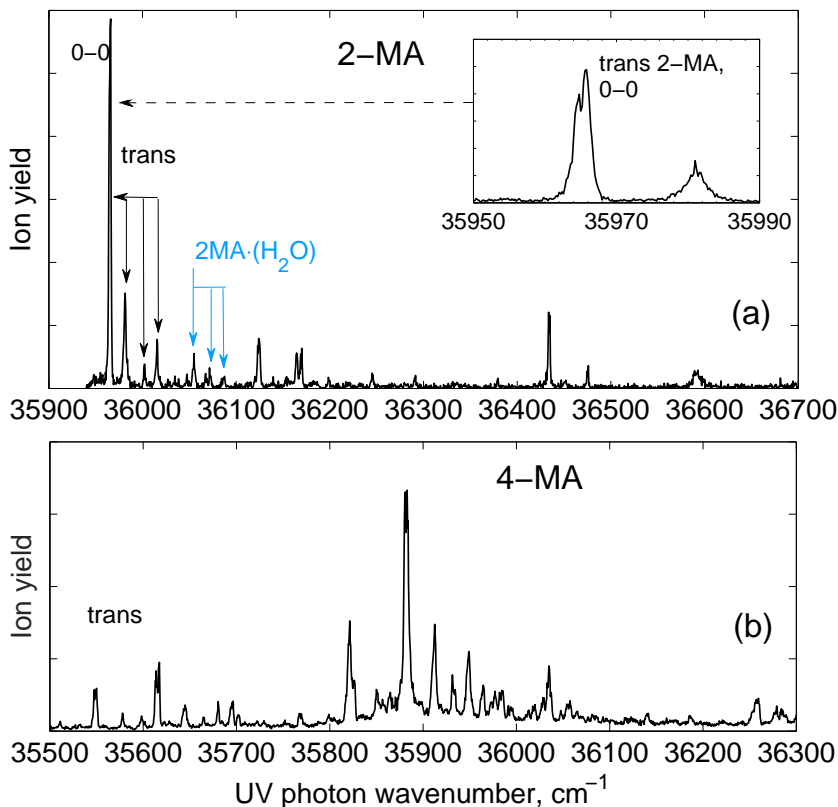


FIG. 2. (1+1)-REMPI spectra of 2-MA (a) and 4-MA (b) molecules. The origin transition of the *trans* conformer of 2-MA is denoted as “0-0”. The peaks marked with blue arrows predominantly originate from UV-induced fragmentation of 2-MA·(H₂O) clusters.

this combination was shown to be accurate for mid-IR²⁹ and far-IR³¹ vibrations of semi-rigid aromatic molecules. The potential energy distribution analysis of vibrational normal modes was performed employing the VEDA4 program³².

IV. RESULTS

A. REMPI spectra

Experimental REMPI spectra of the molecules studied are presented in Fig. 2. The spectrum of 2-MA is dominated by a doublet band with the higher frequency peak at 35965.8 cm⁻¹ (see inset at Fig. 2a). This band was assigned to the origin 0-0 transition of the *trans* conformer, as will be shown in the next section. The split character of the origin band and

the complex low-frequency vibronic pattern in the REMPI spectra were observed earlier for similar molecular systems^{33,34}, and originate from the presence of two populated methyl rotor states of *A* and *E* symmetry in the electronic ground state. The doublet band at 36054 cm⁻¹ and two other bands outlined by blue arrows in Fig. 2a correspond to species different from the *trans* geometry of 2-MA. This was determined by our IR-UV hole-burning measurements, in which the IR wavelength was fixed to a vibrational transition of the *trans* conformer while the UV wavelength was scanned. The IR-UV ion-dip spectrum obtained by tuning the dye laser to these REMPI peaks were identical to that of the 2-MA·(H₂O) clusters which were present in the supersonic-jet molecular beam as verified by measurements of the mass spectrum. Thus we concluded these species to be 2-MA·(H₂O) clusters.

The spectrum of 4-MA in the range of 35500-36300 cm⁻¹ (Fig. 2b) showed many vibrational progression transitions, which most likely originate from the same conformer (*trans*), as supported by our hole-burning measurements. The splitting due to methyl rotor states was observed for several bands, similarly to 2-MA. The intensity of the red-most peaks in the experimental spectrum of 4-MA is lower than the peaks of the blue side. This can either be an indication of a strong geometry change upon electronic excitation (putatively leading to a poor Franck-Condon overlap), or that the origin transition lies well below 35500 cm⁻¹. We performed a time-dependent density functional theory (TD-DFT) geometry optimization³⁵ of the first electronic excited state of *trans* 4-MA, and, indeed, the -CO-NH- moiety altered to non-planar configuration with respect to the ring (with CCNH dihedral of 8.1°), and the torsional angle of para-substituent methyl group changed by $\approx 30^\circ$. It was not possible to determine how such a change in geometry affects the REMPI spectrum in the present experiment, but we plan to study this in detail in the future, as well as how the presence of many methyl rotors affects the REMPI spectrum and its complexity. The IR-UV ion dip spectra presented in the following sections were obtained by probing the origin transition of 2-MA mentioned above, and the vibronic band at 35862 cm⁻¹ of 4-MA.

B. Mid-IR spectra

The mid-IR spectra of the conformers observed of the 2-MA and 4-MA molecules, recorded with the IR-UV ion dip technique, are presented in Fig. 3. The figure also contains theoretical spectra for the stable conformations (Fig. 1), calculated with the anharmonic

VPT2 approach. The comparison with the calculated spectra strongly favors the assignment of the observed conformers of 2-MA and 4-MA to the *trans* geometries. The vibrations of the amide moiety are most intense in this region, with the C=O stretch (Amide I) and NH in plane (i.p.) bending (Amide II and III) observed around 1720, 1520 and 1250 cm^{-1} . The relatively strong vibrational bands observed in the region of 1350-1500 cm^{-1} are due to the deformations of the CH_3 groups. As it can also be seen from Fig. 3, the calculated VPT2 spectra (B3LYP/N07D level of theory) reproduce most of the spectral features, including weaker ones originating from combinational transitions. It is worth noting that the theoretical spectra of the *cis* conformers show some variations with respect to the observed *trans* conformer. Most prominent are the blue-shift of the Amide III band in the case of *cis* geometry, and a strong reduction of the intensity of the Amide II transitions, which become much weaker than the neighboring ring and methyl CH bending vibrations. For the *trans-op* conformer of 2-MA, the calculations predict a weak red-shift of the Amide II and III bands. The vibrational assignments, as well as the comparison between the experimental and calculated frequencies are presented in the supplementary material of this work.

C. Far-IR spectra

The far-IR spectra (220-740 cm^{-1}) of the observed conformers of 2-MA and 4-MA are shown in Figs. 4 and 5, as measured in our IR-UV ion dip experiments. The figures also contain theoretical spectra for all possible conformations, calculated with the anharmonic VPT2 approach. The calculated spectra for the *trans* conformations are in very good agreement with the experimental spectra, thus further supporting the assignment of the observed conformers of 2-MA and 4-MA to the *trans* geometries, made on the basis of the mid-IR data.

The strongest absorption bands in the frequency range of 220-740 cm^{-1} correspond to the fundamental transitions of the Amide V vibration, as classified in the literature⁷. The Amide V vibration is associated with NH out-of-plane (o.p.) bending, with some contributions of the CN torsion motion. In the 2-MA molecule, due to the coupling with the ring vibrations, there are two normal modes of the Amide V character, as suggested by our frequency calculations performed with the B3LYP/N07D method. In the case of the planar *trans* conformation of 2-MA we assigned the strong absorption peaks at 507.5 and 540 cm^{-1} to Amide V bands

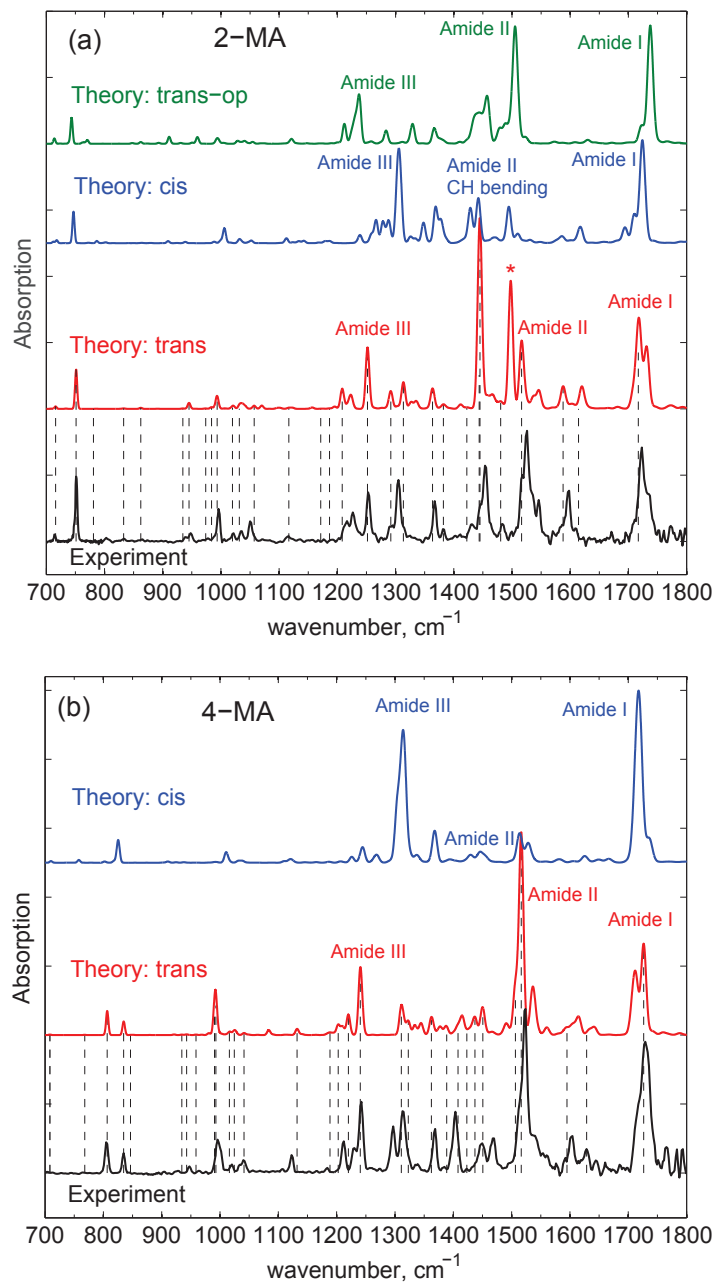


FIG. 3. Experimental mid-IR absorption spectra (in black) of the observed conformers of 2-MA (a) and 4-MA (b), which we assign to the *trans* geometries. The spectra calculated for all possible conformers within the VPT2 anharmonic treatment at the B3LYP/N07D level of theory are shown for comparison. The fundamental theoretical bands of the assigned *trans* conformers are highlighted by vertical dashed lines.

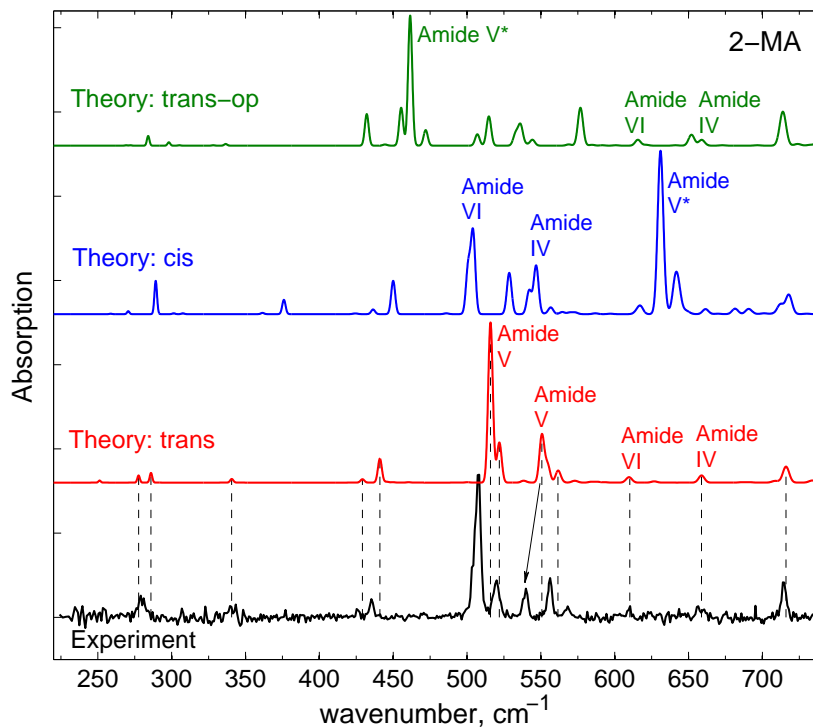


FIG. 4. Experimental far-IR absorption spectra in the range of 220-740 cm^{-1} (in black) for the observed conformer of 2-MA, assigned in this work to the *trans* geometry. The spectra of all possible conformers, calculated with the VPT2 anharmonic treatment at the B3LYP/N07D level of theory, are shown for comparison. The vertical dashed lines denote the position of the fundamental theoretical bands for the *trans* geometry. The marked theoretical NH o.p. bands (Amide V*) were reduced in intensity by a factor of two.

with a small contribution of ring o.p. deformation. The corresponding Amide V bands of the non-planar *trans-op* conformation were calculated to be red-shifted with respect to the planar *trans* geometry and located at 461.5 and 533 cm^{-1} . The second band at 533 cm^{-1} is, however, purely due to the ring o.p. motion, while the Amide V character is predicted to be present in the CCN deformation band at 432 cm^{-1} . For *trans* 4-MA, the Amide V band was observed at 512 cm^{-1} , while the stronger band at 501 cm^{-1} is due to the ring o.p. deformation motion. Interestingly, for the *cis* geometry of the peptide link, the calculations predict a strong blue-shift ($> 100 \text{ cm}^{-1}$) of the Amide V bands with respect to the *trans* geometry. All far-IR vibrations associated with the peptide -CO-NH- moiety, observed and calculated for the 2-MA and 4-MA molecules, are listed in Table I.

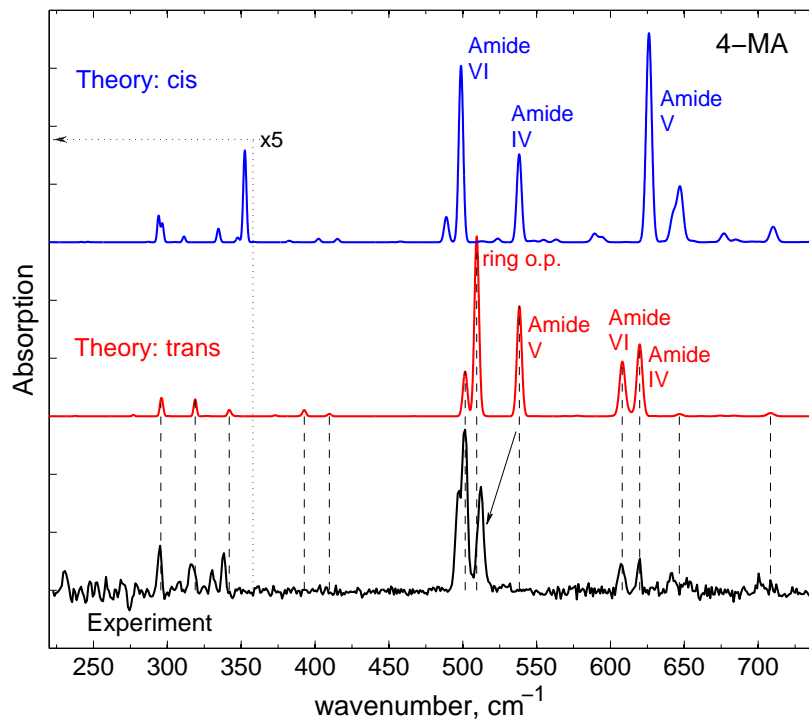


FIG. 5. Experimental far-IR absorption spectra in the range of 220-740 cm^{-1} (in black) for the observed conformer of 4-MA, assigned in this work to the *trans* geometry. The spectra of all possible conformers, calculated with the VPT2 anharmonic treatment at B3LYP/N07D level of theory, are shown for comparison. The vertical dashed lines denote the position of the fundamental theoretical bands for the *trans* geometry.

The studied frequency range also contains transitions which correspond to Amide IV and VI vibrations of the $-\text{CO}-\text{NH}$ moiety. In the *trans* configuration of the peptide link these bands are weaker than the Amide V ones, while for the *cis* geometry they are predicted to be strong. Amide IV is associated with the CO i.p. bending and CC stretch motions, with a small contribution from CNC deformation (see Fig. 1b). Amide VI involves CO o.p. bending, with some o.p. displacement of the NH group. In the experimental spectra of *trans* 2-MA the Amide IV and VI bands appeared at 656 and 610 cm^{-1} , respectively, which is in good agreement with the theoretical data. The calculated frequencies of the same bands in the case of the non-planar *trans-op* conformer only slightly deviate from the *trans* one. In the 4-MA isomer, the Amide IV and VI bands for the *trans* geometry appeared at 620 and 607 cm^{-1} , respectively, hence indicating the red-shift with respect to the 2-MA isomer.

The shift is most likely due to the different reduced masses of the corresponding normal modes in different isomers. The Amide IV and VI bands of both 2-MA and 4-MA in the *cis* configuration are calculated to be strongly red-shifted and enhanced in intensity compared with the *trans* data.

Other characteristic vibrations of the peptide -CO-NH- moiety in the far-IR are associated with CCO i.p. bending, and CCN (or CNC) i.p. bending (see Table I). These vibrations have non-local nature, and for the 2-MA and 4-MA in the *trans* geometry they show variations in frequency, mostly due to the contributions from other types of the phenyl ring and methyl group motions. Among the CCN and CNC i.p. bending vibrations of the *trans* and *trans-op* geometries of 2-MA, only CNC deformation with the methyl i.p. bending are expected to have significant variations in frequency (see Table I). However, according to the calculations for the *cis* geometry, the CCN deformation vibrations show some variations with respect to the *trans* geometry of 2-MA and 4-MA.

V. DISCUSSION

First, we shall discuss the predominant abundance of the *trans* conformations of the 2-MA and 4-MA molecules, and absence of other conformations in our supersonic-jet experiments. The literature data for similar molecular systems include several gas-phase studies on the conformational preferences of the peptide -CO-NH- moiety in *N*-phenylamides^{33,37-41}. Among them, the formanilide molecule with a hydrogen attached to the CO group was observed in both the *trans* and *cis* configurations^{33,37,38}, with the *trans* conformation being more abundant than *cis* (93.5 % and 6.5 % abundance, respectively). The replacement of the amidic hydrogen with a methyl group in *N*-methylformanilide led to an increased abundance of the *cis* geometry, but also the *trans* amide group was twisted out of plane with respect to the phenyl ring³³. For the acetanilide molecule, with a methyl group attached to the CO group, only the *trans* configuration was detected by vibrationally resolved electronic spectroscopy^{33,37,39}. However, in a subsequent study the *cis* configuration was found with the help of microwave spectroscopy⁴⁰, despite the fact that the *cis* species were twenty times less abundant than the *trans* species.

The 2-MA and 4-MA molecules studied have similar chemical composition to acetanilide, with a difference that the hydrogen atom of the aromatic ring is substituted by a methyl

TABLE I. Experimental and theoretical frequencies of vibrations which are characteristic for the peptide -CO-NH- moiety in 2-MA and 4-MA. The theoretical values are from the VPT2 frequency analysis at the B3LYP/N07D level of theory. The calculated harmonic frequencies and available experimental³⁶ data for N-MethylAcetamide (NMA) and its dimer are shown for comparison.

	<i>trans</i> 2-MA		<i>trans-op</i> 2-MA		<i>cis</i> 2-MA		<i>trans</i> 4-MA		<i>cis</i> 4-MA		NMA		NMA dimer	
	exp	theory	exp	theory	exp	theory	exp	theory	exp	theory	exp	theory	exp	theory
Amide IV	656	658.8	–	659.0	–	546.8	620	619.8	–	538.2	619 ^a	623.0	–	624.9
											–	627.9		
Amide VI	610	610.2	–	615.7	–	504.1	607	608.0	–	498.8	658 ^a	630.8	–	597.6
											–	630.0		
Amide V	507.5	515.9	–	461.5	–	631.0	512	538.3	–	626.1	439 ^a	458.6	–	716.9
	540	550.7	–	–	–	641.0	–	–	–	645.5	–	–	–	423.8
CCO i.p. bend	556	561.6	–	576.8	–	556.7	–	–	–	589.2	–	–	–	–
CCN def.	520	521.9	–	514.8	–	500.8	497	501.6	–	488.9	–	–	–	–
	426	429.2	–	432.1 ^b	–	436.4	–	392.7	–	402.4	429 ^a	433.7	–	–
	340	340.6	–	336.6	–	376.0	316	318.9	–	352.2	279 ^a	287.0	–	–
CNC def.+CH ₃	279	277.6	–	298.1	–	270.6	294.5	295.6	–	296.6	–	–	–	–
i.p. bending														
CNC def.+CH ₃	282	286.0	–	284.1	–	289.2	338	341.9	–	334.6	–	–	–	–
o.p. bending														

^a From Ref.³⁶

^b This CCN deformation vibration of *trans-op* 2-MA also has a small Amide V contribution

group in the *ortho*- and *para*-position, respectively. Similar to acetanilide, the gas-phase 2-MA and 4-MA molecules adopt preferentially the *trans* conformation as indicated by our IR-UV ion-dip and hole-burning measurements, as well as verified by the theoretical calculations (Figs. 3-5). The hole-burning measurements performed for 2-MA and 4-MA identified only the *trans* conformers. Moreover, the search for 2-MA REMPI transitions in the range of 35200-36700 cm⁻¹ did not show any peaks originating from other conformers than *trans*.

According to our DFT calculations at the B3LYP/N07D level, for the *trans* geometry of 4-MA the amide group is planar with respect to the ring, and the hydrogen of the *para*-methyl group has a CCCH dihedral angle of 90° (Fig. 1). The *cis* geometry is also stable, but it is 10.6 kJ/mol higher in energy than the *trans* geometry, which can result in a very low abundance in our gas-phase measurements. In the case of 2-MA, three different stable geometries are possible: the planar *trans* is most stable, the non-planar *trans-op* is higher in energy by 6 kJ/mol, and *cis* is even higher by 8.15 kJ/mol (B3LYP/N07D level). Similar to the case of 4-MA, the *trans-op* and *cis* conformers of 2-MA can have a low abundance, despite that their energies above the planar *trans* structure are lower than in 4-MA. The amide moiety of the *trans-op* conformer is twisted out of plane with respect to the phenyl ring by $\approx 60^\circ$, due to steric interactions between the adjacent carbonyl oxygen and the methyl group in the *ortho*-position. The amide moiety in the *cis* configuration of the peptide link is also twisted out of plane by $\approx 48^\circ$ for both 2-MA and 4-MA. The reason for this is a steric interaction between the methyl group and the hydrogen atom of the phenyl ring.

The measured far-IR spectra of the observed *trans* conformations of 2-MA and 4-MA are in very good agreement with the DFT frequency calculations based on the anharmonic VPT2 approach. This further confirms our theoretical data obtained for the other conformations, which we can use for a comparative analysis, at least qualitatively, between the vibrational signatures of the different conformations. For example, the Amide V band in the *trans-op* geometry of 2-MA is predicted to be red-shifted by $\approx 50 \text{ cm}^{-1}$ versus the *trans* geometry, which correlates with the structural differences between the two conformations. First, due to the resonance interactions between the ring and -CO-NH- moiety in the case of the planar *trans* conformation, the force constants of NH o.p. bending motion are increased, because this vibration distorts the resonantly stabilized planar geometry. The *trans-op* conformation, however, has a twisted geometry ($\approx 60^\circ$) of the acetamide group with respect to the aromatic ring, and hence the force constants are lower. Second, the -CO-NH- moiety in the *trans-op* conformation deviates from planarity by $\approx 10^\circ$ (B3LYP/N07D geometry) thus further reducing the force constants. Such deviations from planarity may also take place in polypeptide structures^{25,26}, and the Amide V vibrations might be very diagnostic in order to study them. Moreover, in the case of weak NH $\cdots\pi$ interactions between the aromatic groups of amino acids and nearby amide hydrogen⁴², the Amide V vibration can be diagnostic as well.

The frequency calculations show that the Amide V bands of the *cis* isomers are strongly blue-shifted with respect to the *trans* isomer, by 123.5 and 88 cm^{-1} for 2-MA and 4-MA, respectively (see Figs. 4-5 and Table I). Moreover, the Amide IV and VI bands of the *cis* form are predicted to be strongly red-shifted compared with the *trans* form. Such changes in the fundamental Amide frequencies most likely originate from the different geometry of the peptide link and reduced masses of the corresponding normal modes. It is worth noting that the Amide V frequency of the *cis* peptide link itself, as calculated for the model molecule NMA, is higher than for the *trans* form by 54 cm^{-1} (at B3LYP/N07D level). Moreover, the optimized geometries of the *cis* 2-MA and 4-MA show that the aromatic ring induces the geometric constraints which reduce the distance between the O and H atoms of the peptide moiety to 2.365 and 2.369 Å correspondingly, in comparison with the *cis*-NMA value of 2.415 Å. This structural change can be a reason for the shifts of the Amide IV-VI bands. The large differences between the Amide IV-VI bands of *trans* and *cis* isomers indicate that far-IR spectroscopy can be used to analyze the fraction of *cis*-type peptide links. Despite the fact that the majority of the peptide links in proteins and peptides are of *trans*-type, this finding can be important for the structural characterization of cyclic peptides, where links of the *cis*-type can be present⁴³⁻⁴⁸. In the current study it was not possible to measure the far-IR spectrum of the 2-MA *cis* conformer because of its low abundance under the supersonic jet conditions. A potential candidate for future studies of the sensitivity of the far-IR Amide bands is a formamide molecule, which was observed both in *trans* and *cis* form³⁷. The dipeptide Phe-Ser in linear and cyclic form⁴⁷ is another candidate for such investigations.

The most abundant secondary structures in peptides and proteins such as α -helices and β -sheets are stabilized by hydrogen bonding ($\text{NH}\cdots\text{O}=\text{C}$). Thus, most of the Amide bands in peptides are altered by the presence of hydrogen bonding, *e.g.* the Amide I bands manifest a red-shift in frequency, while Amide II-III show a blue-shift. To study the effect of hydrogen bonding on the Amide IV-VI bands we performed frequency calculations on a simple peptide model molecule, NMA, and its hydrogen bonded dimers and trimers. The theoretical results for NMA-dimer show that upon $\text{NH}\cdots\text{O}=\text{C}$ hydrogen bonding the Amide V frequency shifts to the blue by 258 cm^{-1} , from 459 to 717 cm^{-1} at the B3LYP/N07D level of theory, which amounts to more than 50% of the frequency of the NMA-monomer without hydrogen bonding. The corresponding blue-shift for the NMA-trimer with two hydrogen bonds is even larger, 294 cm^{-1} . These results are also supported by available experimental

data on matrix and condensed-phase spectra for NMA^{7,36,49,50}. Such a large alternation in the frequency of the Amide V band makes it a very promising candidate for an accurate determination of both secondary structures of polypeptides and the strength of the hydrogen bonds involved.

VI. CONCLUSIONS

In this work an experimental study of low-frequency vibrations of isolated 2- and 4-MethylAcetanilide molecules was combined with anharmonic VPT2 calculations. The planar geometries with the *trans* configuration of the peptide link were found to be strongly favored under the supersonic-jet expansion conditions. The experimental and theoretical data show that the Amide IV-VI vibrations of the -CO-NH- moiety can be very sensitive to the structure of the peptide link and the molecular backbone, further supporting the previously demonstrated conformer-specificity of such vibrations²³. For the *cis*-configuration of the -CO-NH- moiety our calculations predict a strong blue-shift of the Amide V bands with respect to the *trans* geometry, and a strong red-shift of the Amide IV and VI bands. This feature can enable a far-IR characterization of cyclic peptides where the *cis*-peptide links can exist. Furthermore, the Amide V vibration manifests strong blue-shifts upon hydrogen bond formation on the NH moiety, thus being a sensitive characteristic of the hydrogen bond strength and secondary structures of polypeptides stabilized by hydrogen bonding.

VII. SUPPLEMENTARY MATERIAL

The supplementary material contains experimental and theoretical vibrational frequencies of the *trans* 2-MA and 4-MA conformers observed experimentally, as well as theoretical frequencies for the *trans-op* conformer of 2-MA. The theoretical analysis is performed in the harmonic approximation and with the VPT2 approach using the B3LYP/N07D level of theory.

VIII. ACKNOWLEDGMENTS

We acknowledge the Swedish Research Council (VR) (Grant No. 621-2011-4043), the Knut and Alice Wallenberg Foundation (Sweden) and the Dutch Foundation for Funda-

mental Research on Matter (FOM) for financial support. The research leading to these results has received funding from the European Community's Seventh Framework Programme (FP7/2007-2013) under grant agreement No. 312284. The authors highly appreciate the skillful assistance of the staff at the FELIX laboratory. The calculations were sponsored by NWO Physical Sciences (EW) by granting access to the supercomputer facilities at SurfSara (project no. MP-264-13).

REFERENCES

- ¹A. M. Rijs and J. Oomens, eds., *Gas-Phase IR Spectroscopy and Structure of Biological Molecules*, Vol. 364 (Top. Curr. Chem., 2015) pp. 1–406, and references therein.
- ²D. J. Bakker, A. Peters, V. Yatsyna, V. Zhaunerchyk, and A. M. Rijs, *The Journal of Physical Chemistry Letters* **7**, 1238 (2016).
- ³R. J. Falconer and A. G. Markelz, *Journal of Infrared, Millimeter, and Terahertz Waves* **33**, 973 (2012).
- ⁴T. Ding, A. P. Middelberg, T. Huber, and R. J. Falconer, *Vibrational Spectroscopy* **61**, 144 (2012).
- ⁵S. Perticaroli, D. Russo, M. Paolantoni, M. A. Gonzalez, P. Sassi, J. D. Nickels, G. Ehlers, L. Comez, E. Pellegrini, D. Fioretto, and A. Morresi, *Phys. Chem. Chem. Phys.* **17**, 11423 (2015).
- ⁶B. Born, S. J. Kim, S. Ebbinghaus, M. Gruebele, and M. Havenith, *Faraday Discuss.* **141**, 161 (2009).
- ⁷J. Bandekar, *Biochimica et Biophysica Acta (BBA) - Protein Structure and Molecular Enzymology* **1120**, 123 (1992).
- ⁸T. Miyazawa, K. Fukusima, S. Sugano, and Y. Masuda, in *Conformation of Biopolymers*, edited by G. Ramachandran (Academic Press, 1967) pp. 557 – 568.
- ⁹Y. Masuda, K. Fukushima, T. Fujii, and T. Miyazawa, *Biopolymers* **8**, 91 (1969).
- ¹⁰K. Itoh, T. Nakahara, T. Shimanouchi, M. Oya, K. Uno, and Y. Iwakura, *Biopolymers* **6**, 1759 (1968).
- ¹¹K. Itoh, T. Shimanouchi, and M. Oya, *Biopolymers* **7**, 649 (1969).
- ¹²K. Itoh, M. Oya, and T. Shimanouchi, *Biopolymers* **11**, 1137 (1972).
- ¹³K. Itoh and H. Katabuchi, *Biopolymers* **11**, 1593 (1972).

- ¹⁴K. Itoh and H. Katabuchi, *Biopolymers* **12**, 921 (1973).
- ¹⁵J. Bandekar and G. Zundel, *Spectrochimica Acta Part A: Molecular Spectroscopy* **38**, 815 (1982).
- ¹⁶H. Kellouai, M. Barthes, G. Page, J. Moret, and J. L. Sauvajol, *Journal of Biological Physics* **21**, 25 (1995).
- ¹⁷P. Papanek, J. E. Fischer, and N. S. Murthy, *Macromolecules* **35**, 4175 (2002).
- ¹⁸T. Ding, T. Huber, A. P. Middelberg, and R. J. Falconer, *The Journal of Physical Chemistry A* **115**, 11559 (2011).
- ¹⁹P. Carcabal, R. T. Kroemer, L. C. Snoek, J. P. Simons, J. M. Bakker, I. Compagnon, G. Meijer, and G. v. Helden, *Phys. Chem. Chem. Phys.* **6**, 4546 (2004).
- ²⁰J. M. Bakker, L. M. Aleese, G. Meijer, and G. von Helden, *Phys. Rev. Lett.* **91**, 203003 (2003).
- ²¹M. Cirtog, A. M. Rijs, Y. Loquais, V. Brenner, B. Tardivel, E. Gloaguen, and M. Mons, *The Journal of Physical Chemistry Letters* **3**, 3307 (2012).
- ²²S. Jaecx, J. Oomens, A. Cimas, M.-P. Gageot, and A. M. Rijs, *Angew. Chem. Int. Ed.* **53**, 3663 (2014).
- ²³J. Mahe, S. Jaecx, A. M. Rijs, and M.-P. Gageot, *Phys. Chem. Chem. Phys.* **17**, 25905 (2015).
- ²⁴M.-P. Gageot, *Phys. Chem. Chem. Phys.* **12**, 3336 (2010).
- ²⁵D. S. Berkholz, C. M. Driggers, M. V. Shapovalov, R. L. Dunbrack, and P. A. Karplus, *Proceedings of the National Academy of Science* **109**, 449 (2012).
- ²⁶R. Improta, L. Vitagliano, and L. Esposito, *PLoS ONE* **6**, 1 (2011).
- ²⁷A. M. Rijs and J. Oomens, *IR Spectroscopic Techniques to Study Isolated Biomolecules*, Vol. 364 (Top. Curr. Chem., 2015) pp. 1–42.
- ²⁸M. J. Frisch, G. W. Trucks, H. B. Schlegel, G. E. Scuseria, M. A. Robb, J. R. Cheeseman, G. Scalmani, V. Barone, B. Mennucci, G. A. Petersson, H. Nakatsuji, M. Caricato, X. Li, H. P. Hratchian, A. F. Izmaylov, J. Bloino, G. Zheng, J. L. Sonnenberg, M. Hada, M. Ehara, K. Toyota, R. Fukuda, J. Hasegawa, M. Ishida, T. Nakajima, Y. Honda, O. Kitao, H. Nakai, T. Vreven, J. A. Montgomery, Jr., J. E. Peralta, F. Ogliaro, M. Bearpark, J. J. Heyd, E. Brothers, K. N. Kudin, V. N. Staroverov, R. Kobayashi, J. Normand, K. Raghavachari, A. Rendell, J. C. Burant, S. S. Iyengar, J. Tomasi, M. Cossi, N. Rega, J. M. Millam, M. Klene, J. E. Knox, J. B. Cross, V. Bakken, C. Adamo, J. Jaramillo,

- R. Gomperts, R. E. Stratmann, O. Yazyev, A. J. Austin, R. Cammi, C. Pomelli, J. W. Ochterski, R. L. Martin, K. Morokuma, V. G. Zakrzewski, G. A. Voth, P. Salvador, J. J. Dannenberg, S. Dapprich, A. D. Daniels, Ö. Farkas, J. B. Foresman, J. V. Ortiz, J. Cioslowski, and D. J. Fox, "Gaussian 09 Revision D.01," Gaussian Inc. Wallingford CT 2009.
- ²⁹V. Barone, M. Biczysko, and J. Bloino, *Phys. Chem. Chem. Phys.* **16**, 1759 (2014), and references therein.
- ³⁰V. Barone, P. Cimino, and E. Stendardo, *J. Chem. Theory Comput.* **4**, 751 (2008).
- ³¹V. Yatsyna, D. J. Bakker, R. Feifel, A. M. Rijs, and V. Zhaunerchyk, *Phys. Chem. Chem. Phys.* **18**, 6275 (2016).
- ³²M. H. Jamroz, *Spectrochim. Acta, Part A* **114**, 220 (2013).
- ³³V. P. Manea, K. J. Wilson, and J. R. Cable, *Journal of the American Chemical Society* **119**, 2033 (1997).
- ³⁴W. Y. Sohn, S.-i. Ishiuchi, M. Miyazaki, J. Kang, S. Lee, A. Min, M. Y. Choi, H. Kang, and M. Fujii, *Phys. Chem. Chem. Phys.* **15**, 957 (2013).
- ³⁵F. Furche and R. Ahlrichs, *The Journal of Chemical Physics* **117**, 7433 (2002).
- ³⁶S. Ataka, H. Takeuchi, and M. Tasumi, *Journal of Molecular Structure* **113**, 147 (1984).
- ³⁷M. Miyazaki, J. Saikawa, H. Ishizuki, T. Taira, and M. Fujii, *Phys. Chem. Chem. Phys.* **11**, 6098 (2009).
- ³⁸J. A. Dickinson, M. R. Hockridge, E. G. Robertso, , and J. P. Simons, *The Journal of Physical Chemistry A* **103**, 6938 (1999).
- ³⁹S. Ullrich, , and K. Müller-Dethlefs, *The Journal of Physical Chemistry A* **106**, 9181 (2002).
- ⁴⁰C. Cabezas, M. Varela, W. Caminati, S. Mata, J. Lopez, and J. Alonso, *Journal of Molecular Spectroscopy* **268**, 42 (2011).
- ⁴¹M. Varela, C. Cabezas, J. C. Lopez, and J. L. Alonso, *The Journal of Physical Chemistry A* **117**, 13275 (2013).
- ⁴²G. Toth, C. R. Watts, R. F. Murphy, and S. Lovas, *Proteins: Structure, Function, and Bioinformatics* **43**, 373 (2001).
- ⁴³D. F. Mierke, T. Yamazaki, O. E. Said-Nejad, E. R. Felder, and M. Goodman, *Journal of the American Chemical Society* **111**, 6847 (1989).

- ⁴⁴M. T. Oakley and R. L. Johnston, *Journal of Chemical Theory and Computation* **9**, 650 (2013).
- ⁴⁵S. Wiedemann, A. Metsala, D. Nolting, and R. Weinkauff, *Phys. Chem. Chem. Phys.* **6**, 2641 (2004).
- ⁴⁶A. P. Wickrama Arachchilage, F. Wang, V. Feyer, O. Plekan, and K. C. Prince, *The Journal of Chemical Physics* **136**, 124301 (2012).
- ⁴⁷A. G. Abo-Riziq, B. Crews, J. E. Bushnell, M. P. Callahan, and M. S. D. Vries, *Molecular Physics* **103**, 1491 (2005).
- ⁴⁸K. Schwing, C. Reyheller, A. Schaly, S. Kubik, and M. Gerhards, *ChemPhysChem* **12**, 1981 (2011).
- ⁴⁹F. Fillaux and M. Baron, *Chemical Physics* **62**, 275 (1981).
- ⁵⁰W. A. Herrebout, K. Clou, and H. O. Desseyn, *The Journal of Physical Chemistry A* **105**, 4865 (2001).